JACS
JOURNAL OF THE AMERICAN CHEMICAL SOCIETY
pubs.acs.org/JACS
Article

Supramolecular Relay-Control of Organocatalysis with a Hemithioindigo-Based Molecular Motor

Kerstin Grill and Henry Dube*

Cite This: https://dx.doi.org/10.1021/jacs.0c09519

ABSTRACT: Integration of individual molecular components such as molecular motors or switches into larger meta-functional systems represents a current challenge at the forefront of molecular machine research. Here we present a modular supramolecular approach to relay the photoinduced geometry changes of a hemithioindigo based molecular motor into catalytic efficiency of a chemical reaction. Using the intrinsic chemical nature of the motor for recognition of different hydrogen-bonding organocatalysts a greater than 10-fold modulation in binding affinity is achieved upon photoisomerization. This change in affinity is then translated effectively into control of catalytic competence of the organocatalysts without direct interference by the motor. As an example the organocatalysed Michael addition reaction between nitrostyrene and 3-methoxy-dimethyl aniline was modulated in situ by visible light irradiation. Thus, dynamic and reversible remote control of catalytic processes by the switching capacity of a hemithioindigo molecular motor is established in a multicomponent chemical system. The high intrinsic modularity of this approach presents further advantages, e.g., for easy tailoring of conditions or facile exchange of catalysts and reactions. These results represent a first stepping stone into integrated chemical networks regulated by molecular machines in a fully dynamic way.

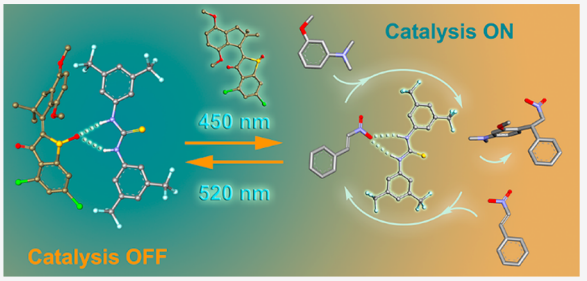

INTRODUCTION

Molecular motors[1−4] represent unique nanoscopic devices[5−7] able to convert external energy input into directional motions at very small scales. To date a variety of molecular motors are available, powered by different energy sources,[2,8−11] performing different kinds of directional motions,[2,12−20] and operating by distinct mechanisms. We have contributed to these developments with visible light responsive molecular motors that are based on the hemithioindigo (HTI) chromophore[21−24] and undergo directional rotational motions.[25−29] Most recently we presented a molecular motor able to deliver a fully directional eight-shaped motion upon green light irradiation.[30] The next frontier of research is presently headed toward application of molecular motors and integration of their functions with other molecular components. Different approaches are followed, e.g., the implementation of molecular motors into supramolecular assemblies,[31] polymers,[32−34] or liquid crystals[35,36] to amplify their motions to larger scales or the direct translation of directional motions to remote motions of other molecular entities.[37−39] Another interesting idea in this context is the use of synthetic molecular motors to interfere with catalytic processes. Effective synthetic examples are represented by the covalent attachment of catalytic moieties to light driven molecular motors enabling control over stereoselectivity of the products.[40,41] In this context a variety of molecular machines and switches with the ability to reversibly control catalysis should be mentioned (for selected examples see refs 42−54) as well as an early example of supramolecular relay control by Ueno[55] and more direct approaches to alter reaction dynamics or, e.g., polymerization by external stimuli (see, e.g., refs 56−61).

In this work we present another approach to control catalysis with a molecular motor **1** via a remote and sequential supramolecular process without functionalizing directly the molecular structure of the motor (Figure 1). We demonstrate how the intrinsic chemical nature of HTI molecular motors can be used to dynamically change catalytic performance in solution and how the same motor molecule can control different types of catalysts. The HTI-based molecular motor is shown to bind two different organocatalysts, *Schreiner's* thiourea **2**[62,63] and squaramide **3**,[64] via hydrogen bonding with its sulfoxide oxygen atom inhibiting their function. Upon light-induced *Z* to *E* isomerization of the motor catalyst binding is weakened significantly leading to an increase of catalysis. In this way a novel concept for the versatile supramolecular integration of the switching capacity of a molecular motor into catalytic processes is demonstrated that will open up new avenues for building future integrated nanomachinery.

Received: September 4, 2020

https://dx.doi.org/10.1021/jacs.0c09519
J. Am. Chem. Soc. XXXX, XXX, XXX−XXX

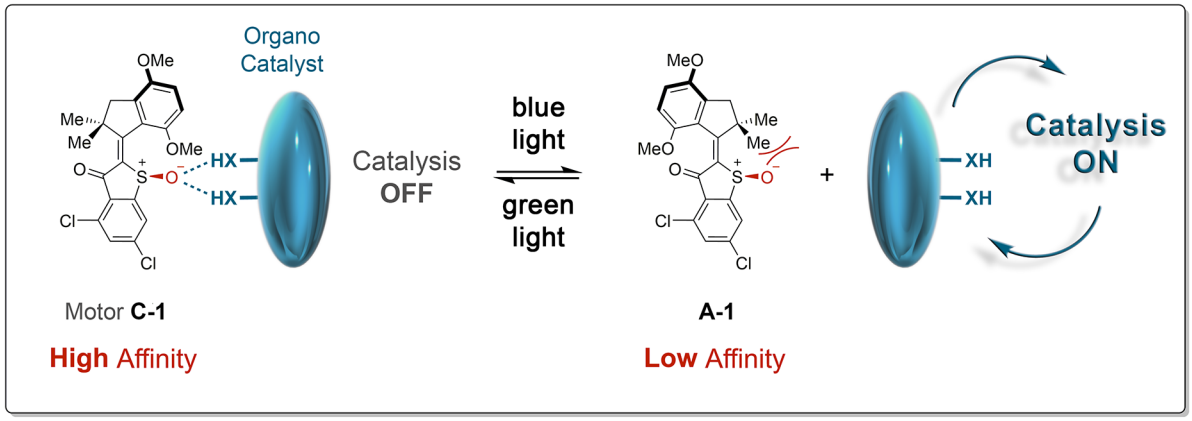

Figure 1. Supramolecular integration of HTI molecular motor **1** to control organocatalysis. In the high-affinity **C** isomeric state different organocatalysts are hydrogen bonded via the sulfoxide oxygen atom leading to hampering of catalysis. Upon visible light irradiation, the low-affinity **A** isomeric state is formed releasing the organocatalyst and switching on catalysis. As selected examples *Schreiner's* thiourea **2** and squaramide **3** organocatalysts were employed for this sequential remote control of reactivity.

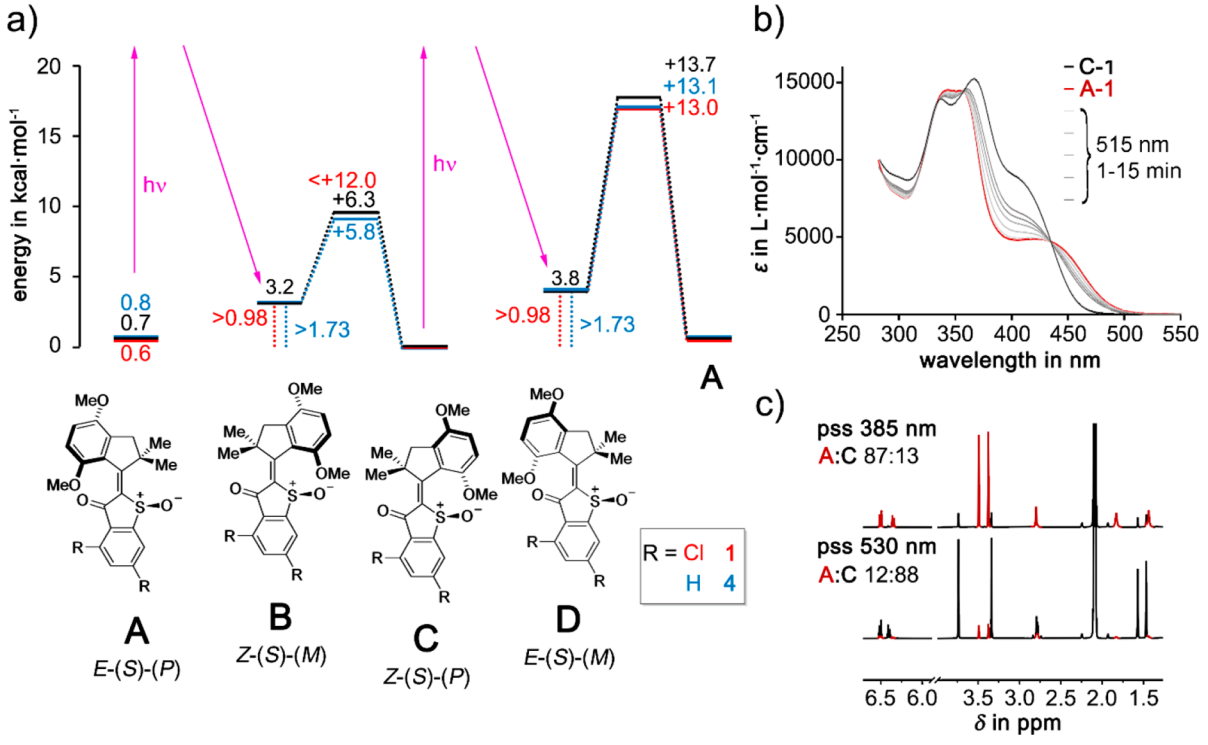

Figure 2. Motor **1** characterization. For clarity only the (*S*)-configured enantiomers are depicted. (a) Assessment of motor function. A mixed theoretical (black) and experimental (red) approach established the energy profile associated with motor **1** operation. The energy profile is very similar to the one obtained for original HTI motor **4** (blue). (b) Molar absorption coefficients of **A-1** (red) and **C-1** (black) and observed spectral changes during photoisomerization (gray). (c) ^{1}H NMR spectra (400 MHz, toluene-d_8, 25 °C) recorded after irradiation to the pss at 385 nm (87% **A-1** enrichment, top) and after irradiation to the pss at 530 nm (88% **C-1** enrichment, bottom).

https://dx.doi.org/10.1021/jacs.0c09519
J. Am. Chem. Soc. XXXX, XXX, XXX−XXX

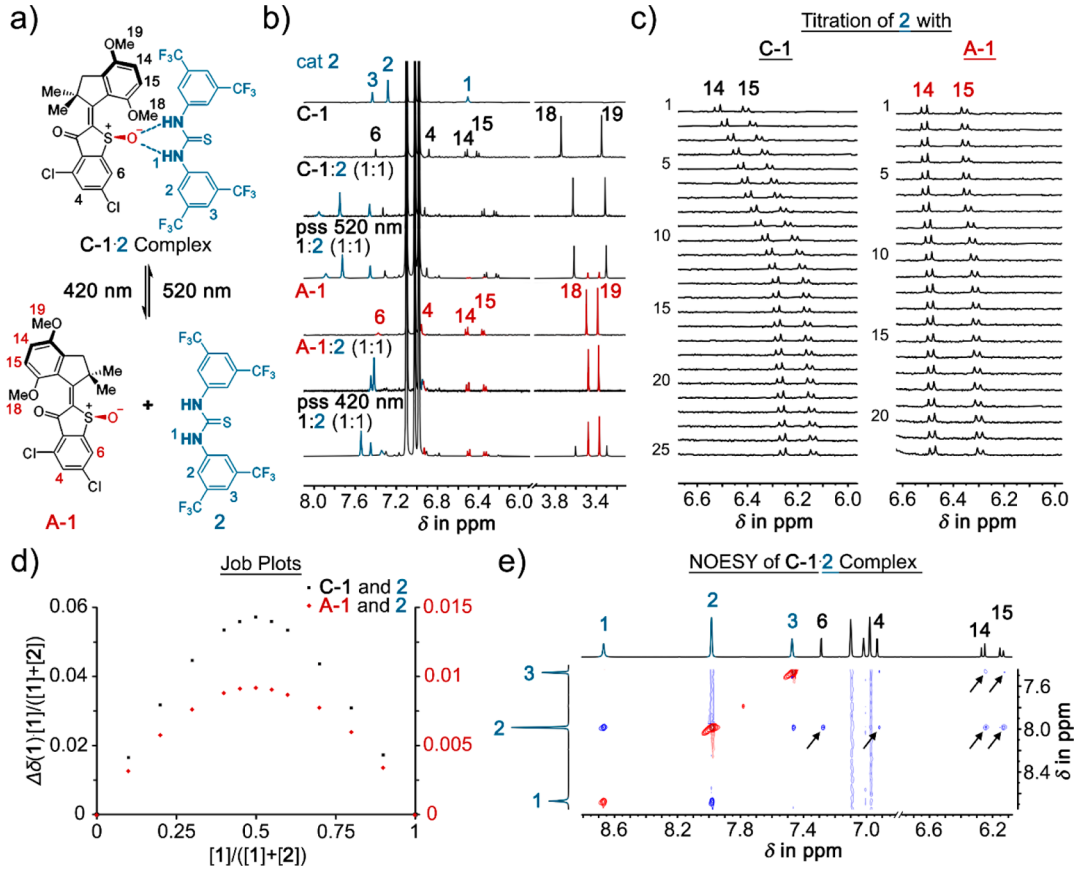

Figure 3. Supramolecular dynamic binding and release of organocatalyst **2** by molecular motor **1** in toluene-d_8 solution. (a) More than 10-fold binding affinity modulation is observed between the **C** and the **A** isomers of **1**. (b) ^{1}H NMR (400 MHz, 30 °C) spectral changes induced by different binding between **C**-**1** or **A**-**1** and **2**. Irradiation with 520 and 420 nm light leads to photoisomerization from the low affinity **A** isomer to the high affinity **C** isomer and vice versa, respectively altering availability of the catalyst in solution. (c) ^{1}H NMR (400 MHz, 30 °C) spectral changes observed during titration of catalyst **2** with **C**-**1** (left) or **A**-**1** (right). (d) Job plot analysis of the binding of catalyst **2** with **C**-**1** (black) or **A**-**1** (red). (e) Partial NOESY NMR spectrum (800 MHz, 30 °C) corroborating information about the binding geometry of the **C**-**1**·**2** complex. Indicative cross signals are marked with arrows.

RESULTS AND DISCUSSION

Assessment of Motor Function. Molecular motor **1** is based on the parent HTI chromophore—an important member of the emerging class of indigoid photoswitches.[65] The synthesis of **1** as precursor molecule was described previously[66] but a full assessment of its motor function has not been undertaken so far. For this reason variable temperature experiments were conducted to obtain a quantitative picture of motor operation (for details of the conformation analysis and elucidation of unidirectionality see the Supporting Information). From this analysis it could be inferred that **1** fully functions as a molecular motor with very similar energetic parameters as the parent original HTI molecular motor **4** (Figure 2a). However, in a preliminary ^{1}H NMR screening it was found that motor **1** shows significantly larger differences between the molecular recognition abilities of its **A** and **C** isomers as compared to the original motor **4**. Motor **1** was therefore chosen as most promising derivative for catalysis control. For the present study it was of additional importance to assess the possible isomer enrichment in the photostationary state (pss) as the two most stable switching states (each in racemic form) **C**-**1** (*Z*-(*S*)-(*P*)/*Z*-(*R*)-(*M*)) and **A**-**1** (*E*-(*S*)-(*P*)/*E*-(*R*)-(*M*)) are further used to control catalysis (Figure 2b,c). Irradiation at different wavelengths was conducted in toluene-d_8 and CD_2Cl_2 solutions as well as in the presence of catalysts and substrates of catalysis. Best performance for photoisomerization of pure motor **1** was observed at 385 nm (87% **A**-**1**) and 530 nm (88% **C**-**1**) irradiations. However, it became apparent that longer wavelength visible light is crucial for proper functioning of the full system, as irradiation with wavelengths of up to 435 nm lead to significant isomerization of the nitro-styrene substrate **5** (see Figure 4 and the catalysis section for the introduction of the catalytic substrates **5** and **6**) and decomposition of catalyst **2**. For these reasons longer wavelengths for the **C** to **A** photoisomerization were used in the latter cases (see below). Another crucial factor for proper performance is thermal stability of the two motor isomers to guarantee nonchanging conditions for the prolonged time of catalysis assessment after switching. Also in this regard motor **1** displayed very beneficial behavior possessing very high thermal bistability with an associated free enthalpy of activation $\Delta G^* > 32$ kcal/mol for the thermal isomerization at 100 °C in toluene-d_8 solution (see the Supporting Information for details). The thermal isomerization kinetics did not change significantly in the presence of organocatalysts and substrates.

Supramolecular Interactions between Motor 1 and Organocatalysts. Next we investigated the supramolecular interactions of motor **1** with organocatalysts (see exemplarily Figure 3a–d and also the Supporting Information for details of the binding assessments). Upon addition of *Schreiner's* thiourea catalyst **2** to the **C** isomers of **1** strong shifts of the motors proton

https://dx.doi.org/10.1021/jacs.0c09519
J. Am. Chem. Soc. XXXX, XXX, XXX−XXX

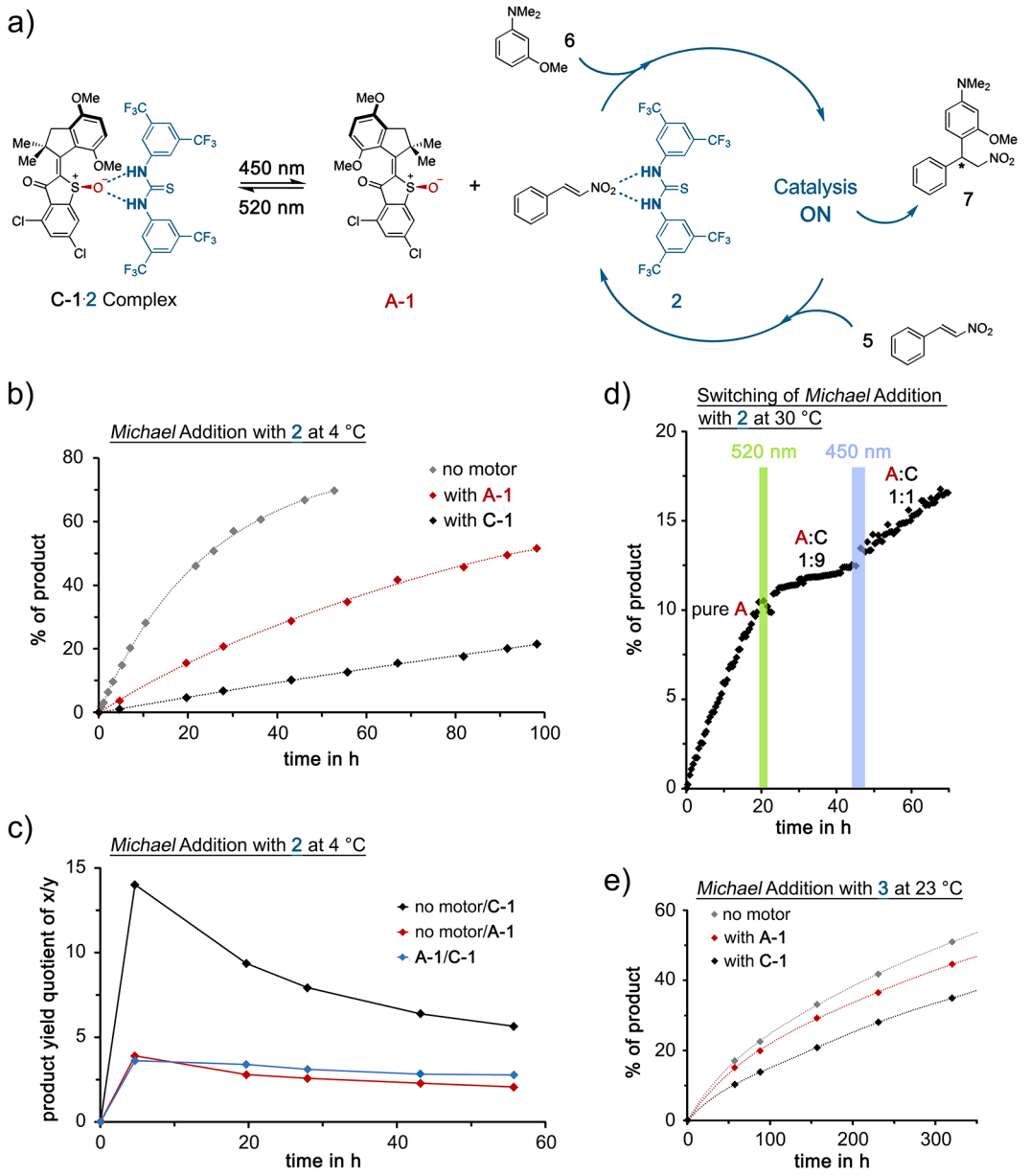

Figure 4. Remote control of organocatalysis by molecular motor **1**. (a) Schematic representation of the remote control using organocatalyst **2**. (b) Difference in catalytic performance when adding either no motor **1** (gray), pure **C-1** (black), or pure **A-1** (red) to the catalytic system of **2**, **5**, and **6** (conditions: **5** = 0.2 M, **6** = 0.3 M, 20 mol % **2**, 20 mol % motor isomer **1**, toluene-d_8, 4 °C). (c) Difference factors in product formation (product yield quotient) for no added motor/added **C-1** (black), no added motor/added **A-1** (red), added **C-1**/added **A-1** (blue) of the catalytic system of **2**, **5**, and **6** (conditions: **5** = 0.2 M, **6** = 0.3 M, 20 mol % **2**, 20 mol % motor isomer **1**, toluene-d_8, 4 °C). (d) In situ light induced remote control of catalytic performance for the catalytic system of **2**, **5**, and **6** (conditions: **5** = 0.1 M, **6** = 0.15 M, 20 mol % **2**, 20 mol % motor isomer **1**, toluene-d_8, 30 °C). Light irradiation steps are illustrated in green and purple after 20 and 45 h reaction times. (e) Difference in catalytic performance when adding either no motor **1** (gray), pure **C-1** (black), or pure **A-1** (red) to the catalytic system of **3**, **5**, and **6** (conditions: **5** = 0.2 M, **6** = 0.3 M, 20 mol % **3**, 20 mol % motor isomer **1**, THF-d_8, 23 °C).

signals in the ^{1}H NMR spectrum (30 °C, toluene-d_8) indicate significant and dynamic binding (Figure 3b). In the corresponding **A** isomeric state of **1** much weaker shifts are observed corroborating much less pronounced supramolecular interactions. A binding constant of K_a = 2300 L mol^{-1} at 30 °C was established by titration of catalyst **2** with motor **C-1** for a 1:1 stoichiometry in toluene-d_8 solution (Figure 3c). The 1:1 stoichiometry was confirmed in an independent Job-plot experiment (Figure 3d). Upon closer analysis with the aid of control experiments and 2D NMR spectroscopy a model for the association between **C-1** and **2** has been developed. Especially indicative are direct NOE cross signals between protons 2 of **2** and the motor proton 6 located in the ortho position with respect to the sulfoxide as well as the aromatic protons 14 and 15 of the indanone rotor fragment (see Figure 3e and the Supporting Information). From these and other NOE signals it can clearly be shown that hydrogen binding of **2** toward **C-1** occurs at the sulfoxide function and that **2** approaches the motor from the sulfoxide side in the supramolecular complex. An additional control experiment was conducted to test the relative affinity of a ketone versus a sulfoxide function. Comparison of the relative influence of catalyst **2** addition to either acetone or

https://dx.doi.org/10.1021/jacs.0c09519
J. Am. Chem. Soc. XXXX, XXX, XXX−XXX

DMSO on the induced proton signal shifts in the ^{1}H NMR spectrum showed clear preference for the sulfoxide as well (for details see the Supporting Information). For the **A** isomer of **1** a significantly weaker association constant of K_a = 200 L mol^{-1} at 30 °C was established by titration again for a 1:1 stoichiometry (Figure 3b,c). Again independent Job-plot experiments confirmed the 1:1 binding stoichiometry (Figure 3d). A similar 2D NMR analysis confirms much weaker interactions involving still mainly the sulfoxide side of **A-1** in the binding (for details see the Supporting Information). Taken together these experiments thus established a greater than 10-fold affinity difference for *Schreiner's* thiourea organocatalyst **2** between the strongly binding **C** isomer and the weakly binding **A** isomer of motor **1**. Similar titration experiments were not possible with the squaramide catalyst **3** because of its very low solubility but a qualitative assessment of induced proton signal shifting upon its addition to **1** in the ^{1}H NMR spectra allowed us to draw similar conclusions: significant association with **C** isomeric **1** and less interactions with the corresponding **A** isomer (see the Supporting Information).

Reversible binding and unbinding upon photoswitching could straight-forwardly be monitored by irradiating a 1:1 mixture of **1** and organocatalyst **2** at different wavelengths until the pss was reached. A maximum of 86% of **C-1** was obtained at 520 nm and a maximum of 78% **A-1** at 420 nm irradiation in the presence of **2**. The corresponding shifts of proton signals proved dynamic binding (**C-1**) and release (**A-1**) of the catalysts in the two switching states, respectively (see Figure 3b). As mentioned above photoswitching at wavelengths up to 420 nm leads to photoisomerization of the nitro-styrene starting material **5** and thus changes the conditions of catalysis. Additionally slight photodegradation is observed below 435 nm irradiation already in binary mixtures of catalyst **2** and motor **1** but mostly at higher concentrations of >1 mM (see the Supporting Information for details). For these reasons photoswitching in the full catalytically competent system including large excesses of starting materials **5** and **6** was done using 450 nm light for the **C-1** to **A-1** photoisomerization direction. At this wavelength a reduced pss containing a maximum of 50−64% of the **A** isomer is obtained.

Assessment of Motor-Remote Controlled Catalysis. For the catalytic process to be remote controlled the *Michael* addition reaction between nitrostyrene **5** and 3-methoxy-dimethyl aniline **6**[67] was chosen (Figure 4a). The reaction progress was monitored at 4 and 30 °C via ^{1}H NMR spectroscopy over the course of hours to days using toluene-d_8 as solvent. This reaction does not proceed in absence of a catalyst so that background reactions are eliminated. Upon addition of *Schreiner's* thiourea catalyst **2** the nitro-group of **5** is bound via hydrogen bonding increasing electrophilicity of the adjacent double bond enough to enable facile reaction within hours at a catalyst loading of 20%. Upon adding 1.0 equiv (with respect to catalyst **2**) of motor **1** in its purely **C** isomeric form catalysis is severely slowed down reaching only a fraction of the conversion within the same time frame. When adding purely **A** isomeric **1** catalysis rate is increased compared to the **C** isomer containing reaction mixture by a factor (product yield quotient) of 2.2 at 30 °C (see Figure 31 in the Supporting Information). When the catalyst effect is plotted in reverse manner (product yield versus time elapsed) the same catalysis conditions (concentration of species) at a certain point are compared. The corresponding factor (time quotient) then represents the difference in time needed to obtain the same product yield, e.g., either in the presence of **C** or in the presence of **A** (see details in the Supporting Information). In this case the factor is 3.0 signifying a three times faster reaction in the presence of **A** versus **C**. The difference in catalytic efficiency is significantly improved to almost a factor of 4 (both, product yield quotient and time quotient) when the temperature is lowered to 4 °C (Figure 4b,c) establishing strong catalytic modulation by the two motor isomers. Despite a highly dynamic binding mode the difference in association affinity between the two isomers of **1** and **2** translates into effective modulation of inhibitory power over catalysis of **2**, however not in a linear fashion. Although more than 10-fold difference in the binding affinity is observed between the **C** and the **A** isomers of motor **1** at 30 °C a 3.0-fold difference (time quotient) in catalytic performance was achieved at the same temperature. An explanation for this behavior is found when calculating the effective concentration of remaining free catalyst in equilibrium from the respective binding constants.[68] In the presence of pure high-affinity **C** isomer the concentration of remaining free catalyst in solution is 0.004 M, which is 10 times less compared to the 0.04 M total concentration of added catalyst. This factor is seen reproduced when comparing the catalysis experiment with no added motor with the one in which pure **C-1** is added (time quotient, see the black trace in Figure 32 in the Supporting Information). In the presence of weakly binding **A-1** the concentration of remaining free catalyst is 0.012 M, which is only a factor of 3.3 less as compared to the catalyst concentration in the experiment without added motor. Again this factor matches quite well with the observed suppression in catalytic performance by a time quotient of 3.4 at the same temperature (see the red trace in Figure 32 in the Supporting Information). The difference in free catalyst concentration when adding **C-1** versus **A-1** is only a factor of 3.0, which is again in good agreement with the observed modulation of catalytic efficiency by a time quotient of 3.0 (see the blue trace in Figure 32 in the Supporting Information). Thus, it becomes clear that bound catalyst in the complex with motor **1** does not participate in catalysis but only the actually free catalyst in solution. At lower temperatures the dynamics of the binding are expected to be reduced while the binding constants should generally increase. As a result the concentrations of free catalyst decrease accordingly but, given the noticeable temperature effect, significantly less so for the weaker binding **A** isomer. This behavior improves the translation of binding affinities to catalytic performance. Because of time limitations the temperature effect was not explored to its fullest potential. Finally, in an independent experiment (Figure 4d), catalysis commenced in the presence of pure **A** isomeric **1** and the faster kinetics of the reaction were followed by ^{1}H NMR spectroscopy for 20 h at 30 °C. In situ photoisomerization with 520 nm light resulted in 90% enrichment of the **C-1** isomer and further monitoring of the reaction kinetics confirmed significantly slowed down kinetics for the next 25 h. Afterward in situ photoisomerization with 450 nm light resulted in generation of 50% **A-1** isomer and a significant increase in the reaction kinetics as followed for another 25 h. In this way it could be shown that the photoisomerization of motor **1** is directly and efficiently relayed first into modulation of binding to catalyst **2** and then into catalytic performance of the reaction between **5** and **6**.

Similar results were found when a different catalyst **3** was used for the same catalytic reaction taking place in THF-d_8 instead of toluene-d_8 for solubility reasons (Figure 4e). Because of the lower extend of binding between **1** and **3** in this solvent modulation of catalytic performance is slightly less pronounced in this case. A 1.5-fold difference in the reaction kinetics

https://dx.doi.org/10.1021/jacs.0c09519
J. Am. Chem. Soc. XXXX, XXX, XXX−XXX

(product quotient) is observed in the presence of **C** versus **A** isomers of motor **1** at 23 °C as compared to 2.2-fold for the combination of **1** and **2** in toluene-d_8 at 30 °C. Again temperature effects are expected to improve performance significantly but were not tested because of time limitations. It should be emphasized at this point that the overall reduction in catalytic performance by addition of motor **1** is less pronounced for both isomers if squaramide **3** is used as a catalyst in THF. Furthermore, a much longer overall time frame of the reaction is observed in this catalytic system because of the weaker catalytic activity of **3** under the altered conditions. With these experiments modularity of the remote catalytic control approach is demonstrated enabling, e.g., tailoring of overall catalysis time frames with the same molecular motor. To increase modulation of catalytic performance, it is clear from these studies that primarily the binding properties have to be improved further, as this is the crucial mechanism to manipulate the amount of active free catalyst in solution.

In summary, we present a highly modular approach to integrate HTI molecular motors into catalytic processes via a supramolecular relay mechanism. The chlorinated molecular motor **1** exhibits more than 10-fold binding affinity modulation with *Schreiner's* thiourea organocatalyst upon visible light induced photoswitching. For this purpose the intrinsic chemical nature of the HTI motor, i.e., its sulfoxide moiety, is directly used for molecular recognition with the catalyst. The affinity modulation is then effectively translated into reversible modulation of catalytic efficiency for a Michael addition reaction. Simple exchange of just the catalyst demonstrates the advantages of this modular approach, e.g., for tuning reaction parameters such as overall rates of catalytic processes. We need to emphasize at this point that unidirectionality of the motor is not yet used to achieve remote catalysis control. With the present study we have made the first step to harness this potential by demonstrating how HTI motor structures can be integrated supramolecularly into catalytic networks. Further elaboration of this idea in our laboratory are currently headed at escalating the number of processes that can be controlled, using directly the motor characteristics for catalysis, as well as translating chiral information from the motor to the reaction products.

■ ASSOCIATED CONTENT

Supporting Information

The Supporting Information is available free of charge at https://pubs.acs.org/doi/10.1021/jacs.0c09519.

Details of synthesis, motor function analysis, conformational analyses, photochemical behavior, theoretical description, supramolecular interactions, catalysis control, and crystal structural data (PDF)

■ AUTHOR INFORMATION

Corresponding Author

Henry Dube − *Department of Chemistry and Center for Integrated Protein Science CIPSM, Ludwig-Maximilians-Universität München, 81377 München, Germany;* orcid.org/0000-0002-5055-9924; Email: henry.dube@fau.de

Author

Kerstin Grill − *Department of Chemistry and Center for Integrated Protein Science CIPSM, Ludwig-Maximilians-Universität München, 81377 München, Germany*

Complete contact information is available at: https://pubs.acs.org/10.1021/jacs.0c09519

Notes

The authors declare no competing financial interest.

■ ACKNOWLEDGMENTS

In memoriam of Rolf Huisgen. H.D. thanks the "Fonds der Chemischen Industrie" for a Liebig fellowship (Li 188/05) and the Deutsche Forschungsgemeinschaft (DFG) for an Emmy Noether fellowship (DU 1414/1-2). K.G. thanks the "Fonds der Chemischen Industrie" for a Chemiefonds fellowship (Do 199/53). We further thank the Deutsche Forschungsgemeinschaft (SFB 749, A12) and the Cluster of Excellence "Center for Integrated Protein Science Munich" (CIPS^{M}) for financial support.

■ REFERENCES

(1) Kassem, S.; van Leeuwen, T.; Lubbe, A. S.; Wilson, M. R.; Feringa, B. L.; Leigh, D. A. Artificial molecular motors. *Chem. Soc. Rev.* **2017**, *46* (9), 2592−2621.

(2) Koumura, N.; Zijlstra, R. W. J.; van Delden, R. A.; Harada, N.; Feringa, B. L. Light-driven monodirectional molecular rotor. *Nature* **1999**, *401*, 152−155.

(3) Baroncini, M.; Silvi, S.; Credi, A. Photo- and Redox-Driven Artificial Molecular Motors. *Chem. Rev.* **2020**, *120*, 200−268.

(4) Roke, D.; Wezenberg, S. J.; Feringa, B. L. Molecular rotary motors: Unidirectional motion around double bonds. *Proc. Natl. Acad. Sci. U. S. A.* **2018**, *115* (38), 9423−9431.

(5) Kay, E. R.; Leigh, D. A.; Zerbetto, F. Synthetic molecular motors and mechanical machines. *Angew. Chem., Int. Ed.* **2007**, *46* (1−2), 72−191.

(6) Erbas-Cakmak, S.; Leigh, D. A.; McTernan, C. T.; Nussbaumer, A. L. Artificial Molecular Machines. *Chem. Rev.* **2015**, *115* (18), 10081−10206.

(7) Aprahamian, I. The Future of Molecular Machines. *ACS Cent. Sci.* **2020**, *6* (3), 347−358.

(8) Hernandez, J. V.; Kay, E. R.; Leigh, D. A. A Reversible Synthetic Rotary Molecular Motor. *Science* **2004**, *306*, 1532−1537.

(9) Fletcher, S. P.; Dumur, F.; Pollard, M. M.; Feringa, B. L. A Reversible, Unidirectional Molecular Rotary Motor Driven by Chemical Energy. *Science* **2005**, *310*, 80−82.

(10) Erbas-Cakmak, S.; Fielden, S. D. P.; Karaca, U.; Leigh, D. A.; McTernan, C. T.; Tetlow, D. J.; Wilson, M. R. Rotary and linear molecular motors driven by pulses of a chemical fuel. *Science* **2017**, *358* (6361), 340−343.

(11) Wilson, M. R.; Sola, J.; Carlone, A.; Goldup, S. M.; Lebrasseur, N.; Leigh, D. A. An autonomous chemically fuelled small-molecule motor. *Nature* **2016**, *534* (7606), 235−240.

(12) Barrell, M. J.; Campana, A. G.; von Delius, M.; Geertsema, E. M.; Leigh, D. A. Light-driven transport of a molecular walker in either direction along a molecular track. *Angew. Chem., Int. Ed.* **2011**, *50* (1), 285−290.

(13) Ragazzon, G.; Baroncini, M.; Silvi, S.; Venturi, M.; Credi, A. Light-powered autonomous and directional molecular motion of a dissipative self-assembling system. *Nat. Nanotechnol.* **2015**, *10*, 70−75.

(14) Kistemaker, H. A.; Stacko, P.; Visser, J.; Feringa, B. L. Unidirectional rotary motion in achiral molecular motors. *Nat. Chem.* **2015**, *7*, 890−896.

(15) Greb, L.; Lehn, J. M. Light-driven molecular motors: imines as four-step or two-step unidirectional rotors. *J. Am. Chem. Soc.* **2014**, *136* (38), 13114−13117.

(16) Greb, L.; Eichhofer, A.; Lehn, J. M. Synthetic Molecular Motors: Thermal N Inversion and Directional Photoinduced CN Bond Rotation of Camphorquinone Imines. *Angew. Chem., Int. Ed.* **2015**, *54*, 14345−14348.

(17) Haberhauer, G. A molecular four-stroke motor. *Angew. Chem., Int. Ed.* **2011**, *50* (28), 6415−6418.
(18) Cheng, C.; McGonigal, P. R.; Schneebeli, S. T.; Li, H.; Vermeulen, N. A.; Ke, C.; Stoddart, J. F. An artificial molecular pump. *Nat. Nanotechnol.* **2015**, *10* (6), 547−553.
(19) Qiu, Y.; Zhang, L.; Pezzato, C.; Feng, Y.; Li, W.; Nguyen, M. T.; Cheng, C.; Shen, D.; Guo, Q. H.; Shi, Y.; Cai, K.; Alsubaie, F. M.; Astumian, R. D.; Stoddart, J. F. A Molecular Dual Pump. *J. Am. Chem. Soc.* **2019**, *141* (44), 17472−17476.
(20) Qiu, Y.; Song, B.; Pezzato, C.; Shen, D.; Liu, W.; Zhang, L.; Feng, Y.; Guo, Q.-H.; Cai, K.; Li, W.; Chen, H.; Nguyen, M. T.; Shi, Y.; Cheng, C.; Astumian, R. D.; Li, X.; Stoddart, J. F. A precise polyrotaxane synthesizer. *Science* **2020**, *368* (6496), 1247−1253.
(21) Friedländer, P. Ueber schwefelhaltige Analoga der Indigogruppe. *Ber. Dtsch. Chem. Ges.* **1906**, *39*, 1060−1066.
(22) Kitzig, S.; Thilemann, M.; Cordes, T.; Rück-Braun, K. Light-Switchable Peptides with a Hemithioindigo Unit: Peptide Design, Photochromism, and Optical Spectroscopy. *ChemPhysChem* **2016**, *17* (9), 1252−1263.
(23) Graupner, F. F.; Herzog, T. T.; Rott, F.; Oesterling, S.; de Vivie-Riedle, R.; Cordes, T.; Zinth, W. Photoisomerization of hemithioindigo compounds: Combining solvent- and substituent- effects into an advanced reaction model. *Chem. Phys.* **2018**, *515*, 614−621.
(24) Wiedbrauk, S.; Dube, H. Hemithioindigo—an emerging photoswitch. *Tetrahedron Lett.* **2015**, *56* (29), 4266−4274.
(25) Guentner, M.; Schildhauer, M.; Thumser, S.; Mayer, P.; Stephenson, D.; Mayer, P. J.; Dube, H. Sunlight-powered kHz rotation of a hemithioindigo-based molecular motor. *Nat. Commun.* **2015**, *6*, 8406.
(26) Huber, L. A.; Hoffmann, K.; Thumser, S.; Böcher, N.; Mayer, P.; Dube, H. Direct Observation of Hemithioindigo-Motor Unidirectionality. *Angew. Chem., Int. Ed.* **2017**, *56*, 14536−14539.
(27) Wilcken, R.; Schildhauer, M.; Rott, F.; Huber, L. A.; Guentner, M.; Thumser, S.; Hoffmann, K.; Oesterling, S.; de Vivie-Riedle, R.; Riedle, E.; Dube, H. Complete Mechanism of Hemithioindigo Motor Rotation. *J. Am. Chem. Soc.* **2018**, *140*, 5311−5318.
(28) Schildhauer, M.; Rott, F.; Thumser, S.; Mayer, P.; de Vivie-Riedle, R.; Dube, H. A Prospective Ultrafast Hemithioindigo Molecular Motor. *ChemPhotoChem.* **2019**, *3*, 365−371.
(29) Gerwien, A.; Mayer, P.; Dube, H. Photon-Only Molecular Motor with Reverse Temperature-Dependent Efficiency. *J. Am. Chem. Soc.* **2018**, *140*, 16442−16445.
(30) Gerwien, A.; Mayer, P.; Dube, H. Green light powered molecular state motor enabling eight-shaped unidirectional rotation. *Nat. Commun.* **2019**, *10* (1), 4449.
(31) Chen, J.; Leung, F. K.; Stuart, M. C. A.; Kajitani, T.; Fukushima, T.; van der Giessen, E.; Feringa, B. L. Artificial muscle-like function from hierarchical supramolecular assembly of photoresponsive molecular motors. *Nat. Chem.* **2018**, *10* (2), 132−138.
(32) Li, Q.; Fuks, G.; Moulin, E.; Maaloum, M.; Rawiso, M.; Kulic, I.; Foy, J. T.; Giuseppone, N. Macroscopic contraction of a gel induced by the integrated motion of light-driven molecular motors. *Nat. Nanotechnol.* **2015**, *10*, 161−165.
(33) Foy, J. T.; Li, Q.; Goujon, A.; Colard-Itte, J.-R.; Fuks, G.; Moulin, E.; Schiffmann, O.; Dattler, D.; Funeriu, D. P.; Giuseppone, N. Dual-light control of nanomachines that integrate motor and modulator subunits. *Nat. Nanotechnol.* **2017**, *12*, 540−545.
(34) van Leeuwen, T.; Heideman, G. H.; Zhao, D.; Wezenberg, S. J.; Feringa, B. L. In situ control of polymer helicity with a non-covalently bound photoresponsive molecular motor dopant. *Chem. Commun.* **2017**, *53* (48), 6393−6396.
(35) Eelkema, R.; Pollard, M. M.; Vicario, J.; Katsonis, N.; Ramon, B. S.; Bastiaansen, C. W.; Broer, D. J.; Feringa, B. L. Molecular machines: nanomotor rotates microscale objects. *Nature* **2006**, *440* (7081), 163.
(36) Orlova, T.; Lancia, F.; Loussert, C.; Iamsaard, S.; Katsonis, N.; Brasselet, E. Revolving supramolecular chiral structures powered by light in nanomotor-doped liquid crystals. *Nat. Nanotechnol.* **2018**, *13*, 304−308.
(37) Štacko, P.; Kistemaker, J. C. M.; van Leeuwen, T.; Chang, M.-C.; Otten, E.; Feringa, B. L. Locked synchronous rotor motion in a molecular motor. *Science* **2017**, *356* (6341), 964−968.
(38) Uhl, E.; Thumser, S.; Mayer, P.; Dube, H. Transmission of Unidirectional Molecular Motor Rotation to a Remote Biaryl Axis. *Angew. Chem., Int. Ed.* **2018**, *57*, 11064−11068.
(39) Uhl, E.; Mayer, P.; Dube, H. Active and Unidirectional Acceleration of Biaryl Rotation by a Molecular Motor. *Angew. Chem., Int. Ed.* **2020**, *59*, 5730−5737.
(40) Wang, J.; Feringa, B. L. Dynamic control of chiral space in a catalytic asymmetric reaction using a molecular motor. *Science* **2011**, *331* (6023), 1429−32.
(41) Pizzolato, S. F.; Štacko, P.; Kistemaker, J. C. M.; van Leeuwen, T.; Feringa, B. L. Phosphoramidite-based photoresponsive ligands displaying multifold transfer of chirality in dynamic enantioselective metal catalysis. *Nat. Catal.* **2020**, 3 (6), 488−496.
(42) Kassem, S.; Lee, A. T. L.; Leigh, D. A.; Marcos, V.; Palmer, L. I.; Pisano, S. Stereodivergent synthesis with a programmable molecular machine. *Nature* **2017**, *549* (7672), 374−378.
(43) De Bo, G.; Gall, M. A. Y.; Kuschel, S.; De Winter, J.; Gerbaux, P.; Leigh, D. A. An artificial molecular machine that builds an asymmetric catalyst. *Nat. Nanotechnol.* **2018**, *13*, 381−385.
(44) De Bo, G.; Leigh, D. A.; McTernan, C. T.; Wang, S. A complementary pair of enantioselective switchable organocatalysts. *Chem. Sci.* **2017**, *8* (10), 7077−7081.
(45) Göstl, R.; Senf, A.; Hecht, S. Remote-controlling chemical reactions by light: Towards chemistry with high spatio-temporal resolution. *Chem. Soc. Rev.* **2014**, *43* (6), 1982−96.
(46) Eisenreich, F.; Kathan, M.; Dallmann, A.; Ihrig, S. P.; Schwaar, T.; Schmidt, B. M.; Hecht, S. A photoswitchable catalyst system for remote-controlled (co)polymerization in situ. *Nat. Catal.* **2018**, *1* (7), 516−522.
(47) Dorel, R.; Feringa, B. L. Photoswitchable catalysis based on the isomerisation of double bonds. *Chem. Commun.* **2019**, *55* (46), 6477−6486.
(48) Sell, H.; Gehl, A.; Plaul, D.; Sonnichsen, F. D.; Schutt, C.; Kohler, F.; Steinborn, K.; Herges, R. Towards a light driven molecular assembler. *Communications Chemistry* **2019**, *2* (1), 1063 DOI: 10.1038/s42004-019-0163-y.
(49) Goswami, A.; Saha, S.; Biswas, P. K.; Schmittel, M. (Nano)-mechanical Motion Triggered by Metal Coordination: from Functional Devices to Networked Multicomponent Catalytic Machinery. *Chem. Rev.* **2020**, *120* (1), 125−199.
(50) Goswami, A.; Paululat, T.; Schmittel, M. Switching Dual Catalysis without Molecular Switch: Using A Multicomponent Information System for Reversible Reconfiguration of Catalytic Machinery. *J. Am. Chem. Soc.* **2019**, *141* (39), 15656−15663.
(51) Biswas, P. K.; Saha, S.; Paululat, T.; Schmittel, M. Rotating Catalysts Are Superior: Suppressing Product Inhibition by Anchimeric Assistance in Four-Component Catalytic Machinery. *J. Am. Chem. Soc.* **2018**, *140* (29), 9038−9041.
(52) Dommaschk, M.; Echavarren, J.; Leigh, D. A.; Marcos, V.; Singleton, T. A. Dynamic Control of Chiral Space Through Local Symmetry Breaking in a Rotaxane Organocatalyst. *Angew. Chem., Int. Ed.* **2019**, *58* (42), 14955−14958.
(53) Biagini, C.; Fielden, S. D. P.; Leigh, D. A.; Schaufelberger, F.; Di Stefano, S.; Thomas, D. Dissipative Catalysis with a Molecular Machine. *Angew. Chem., Int. Ed.* **2019**, *58* (29), 9876−9880.
(54) Osorio-Planes, L.; Rodriguez-Escrich, C.; Pericas, M. A. Photoswitchable thioureas for the external manipulation of catalytic activity. *Org. Lett.* **2014**, *16* (6), 1704−1707.
(55) Ueno, A.; Takahashi, K.; Osa, T. Photoregulation of catalytic activity of β-cyclodextrin by an azo inhibitor. *J. Chem. Soc., Chem. Commun.* **1980**, No. 17, 837−838.
(56) Hiltebrandt, K.; Pauloehrl, T.; Blinco, J. P.; Linkert, K.; Borner, H. G.; Barner-Kowollik, C. lambda-Orthogonal pericyclic macromolecular photoligation. *Angew. Chem., Int. Ed.* **2015**, *54* (9), 2838−43.

https://dx.doi.org/10.1021/jacs.0c09519
J. Am. Chem. Soc. XXXX, XXX, XXX−XXX

(57) Blasco, E.; Wegener, M.; Barner-Kowollik, C. Photochemically Driven Polymeric Network Formation: Synthesis and Applications. *Adv. Mater.* **2017**, *29* (15), 1604005.
(58) Hiltebrandt, K.; Elies, K.; D'hooge, D. R.; Blinco, J. P.; Barner-Kowollik, C. A Light-Activated Reaction Manifold. *J. Am. Chem. Soc.* **2016**, *138* (22), 7048−54.
(59) Spiegel, C. A.; Hippler, M.; Münchinger, A.; Bastmeyer, M.; Barner-Kowollik, C.; Wegener, M.; Blasco, E. 4D Printing at the Microscale. *Adv. Funct. Mater.* **2020**, *30*, 1907615.
(60) Zhao, H.; Sen, S.; Udayabhaskararao, T.; Sawczyk, M.; Kucanda, K.; Manna, D.; Kundu, P. K.; Lee, J. W.; Kral, P.; Klajn, R. Reversible trapping and reaction acceleration within dynamically self-assembling nanoflasks. *Nat. Nanotechnol.* **2016**, *11* (1), 82−8.
(61) Moreno, S.; Sharan, P.; Engelke, J.; Gumz, H.; Boye, S.; Oertel, U.; Wang, P.; Banerjee, S.; Klajn, R.; Voit, B.; Lederer, A.; Appelhans, D. Light-Driven Proton Transfer for Cyclic and Temporal Switching of Enzymatic Nanoreactors. *Small* **2020**, *16*, 2002135.
(62) Schreiner, P. R.; Wittkopp, A. H-Bonding Additives Act Like Lewis Acid Catalysts. *Org. Lett.* **2002**, *4*, 217−220.
(63) Lippert, K. M.; Hof, K.; Gerbig, D.; Ley, D.; Hausmann, H.; Guenther, S.; Schreiner, P. R. Hydrogen-Bonding Thiourea Organocatalysts: The Privileged 3,5-Bis(trifluoromethyl)phenyl Group. *Eur. J. Org. Chem.* **2012**, *2012* (30), 5919−5927.
(64) Rostami, A.; Colin, A.; Li, X. Y.; Chudzinski, M. G.; Lough, A. J.; Taylor, M. S. N, N′-diarylsquaramides: general, high-yielding synthesis and applications in colorimetric anion sensing. *J. Org. Chem.* **2010**, *75* (12), 3983−92.
(65) Petermayer, C.; Dube, H. Indigoid Photoswitches: Visible Light Responsive Molecular Tools. *Acc. Chem. Res.* **2018**, *51* (5), 1153−1163.
(66) Hoffmann, K.; Mayer, P.; Dube, H. A Hemithioindigo Molecular Motor for Metal Surface Attachment. *Org. Biomol. Chem.* **2019**, *17*, 1979−1983.
(67) Ricci, A.; Herrera, R. P.; Dessole, G. H-Bonding Organocatalysed Friedel-Crafts Alkylation of Aromatic and Heteroaromatic Systems with Nitroolefins. *Synlett* **2004**, No. 13, 2374−2378.
(68) Hargrove, A. E.; Zhong, Z.; Sessler, J. L.; Anslyn, E. V. Algorithms for the determination of binding constants and enantiomeric excess in complex host: guest equilibria using optical measurements. *New J. Chem.* **2010**, *34* (2), 348−354.

https://dx.doi.org/10.1021/jacs.0c09519
J. Am. Chem. Soc. XXXX, XXX, XXX−XXX